Heliyon 10 (2024) e27301

Contents lists available at ScienceDirect

Heliyon

journal homepage: www.cell.com/heliyon

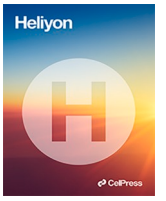

Research article

An ion channel-based prognostic model identified TRPV2 and GJB3 as immunotherapy determinants in pancreatic cancer

Jiakai Mao [a,1], Yu Tian [b,1], Nan Luo [c,*]

[a] Department of Hepatobiliary and Pancreatic Surgery, Department of General Surgery, The Second Hospital of Dalian Medical University, Dalian, Liaoning, China
[b] Department of Vascular Surgery, The Second Hospital of Dalian Medical University, Dalian, Liaoning, China
[c] Department of Infection, The Second Hospital of Dalian Medical University, Dalian, Liaoning, China

ARTICLE INFO

Keywords:
Pancreatic ductal adenocarcinoma
Ion channel genes
Predictive model
Nomogram
Immunotherapy

ABSTRACT

Background: Less than 10% of people who have pancreatic ductal adenocarcinoma (PDAC) will survive the malignancy for five years. The ion channel genes-related biomarker and predictive model were needed for exploitation.
Methods: Differentially expressed ion channel genes (DEICGs) were detected in PDAC patients. GO and KEGG enrichment analysis was conducted on DEICGs. The prognostic genes were found using Cox regression analysis. After that, a risk model was created and examined. A nomogram was created based on independent predictive analysis. The molecular functions of two risk groups were explored. Immune checkpoint molecule expression was compared in two risk groups. We evaluated the possible cancer immunotherapy response in two risk groups using the TIDE method. We further examined how TRPV2 functions in PDAC as a potent oncogene and regulates the activity of macrophages by in vitro validation, including CCK8, EdU, and Transwell assays.
Results: A total of twenty-four DEICGs were found. Next, we discovered that two DEICGs (TRPV2 and GJB3) were connected to PDAC patients' overall survival (OS). The risk model was created and validated, and a nomogram was used to forecast the overall survival of PDAC patients. The high-risk group considerably accumulated oncogenic pathways. Furthermore, we discovered a correlation between the expression of critical immunological checkpoints and the risk score. Furthermore, patients in the high-risk category had a lower chance of benefiting from immune therapy. The HPA database confirmed that TRPV2 is expressed as a protein. Lastly, TRPV2 controls macrophage activity and acts as a potent oncogene in PDAC.
Conclusion: Altogether, this study suggested that two ion channel genes, TRPV2 and GJB3, were potential biomarkers for the prognosis of PDAC and immunotherapy targets, and the research will be crucial for creating novel PDAC treatment targets and predictive molecular indicators.

1. Introduction

By 2030, pancreatic ductal adenocarcinoma (PDAC) is expected to rank second in the United States among cancer-related deaths. Currently ranked seventh globally, PDAC is expected to claim 75,000 lives from cancer. Even worse, in certain nations, the five-year

* Corresponding author.
E-mail address: luonanforeverhom@163.com (N. Luo).
[1] Jiakai Mao and Yu Tian contributed equally to this work.

https://doi.org/10.1016/j.heliyon.2024.e27301
Received 21 December 2023; Received in revised form 27 February 2024; Accepted 27 February 2024
Available online 14 March 2024
2405-8440/© 2024 The Authors. Published by Elsevier Ltd. This is an open access article under the CC BY-NC license (http://creativecommons.org/licenses/by-nc/4.0/).

survival rate from this illness is only 9%, despite advancements in surgical methods, chemotherapeutic regimens, and the use of neo-adjuvant chemoradiotherapy [1]. Thus, to provide a foundation for clinical prognosis and treatment, it is imperative to identify prognostic indicators for PDAC and investigate the molecular targets of immunotherapy.

Membrane proteins called ion channels facilitate ions' passage across biological membranes [2]. According to specific research, ion channels are essential for regulating cell volume, immunological response, muscular contraction, hormone production, gene expression, and cell proliferation. Ion channels are involved in many different biological processes, which explains why the number of human disorders linked to ion channel failure has increased throughout the past few years. Specifically, there is mounting evidence that both voltage- and ligand-gated ion channels play a role in the development and pathophysiology of various human malignancies [3]. Angiogenesis, tumor development, metastasis, and vascular permeability are all associated with transient receptor potential (TRP) channels [4]. Numerous ligand-gated channels, including nicotinic acetylcholine receptors, influence the growth of tumor cells, their programmed cell death, and the formation of new blood vessels [5]. Ion channel genes are involved with pancreatic cancer in earlier research. For example, a high level of MCOLN1 was linked to poor clinical-pathological characteristics and a low survival rate in PDAC patients, indicating a potential function for MCOLN1 in PDAC tumor growth [6]. According to specific research, overexpressing TRPM2 in the PDAC cell line PANC-1 enhanced the potential of the cells to proliferate, invade, and spread [7].

An approach to cancer treatment known as "cancer immunotherapy" targets the patient's immune system [8]. It functions by inducing the immune system to identify and combat cancerous cells [9]. Cancer immunotherapy comes in various forms, such as immune checkpoint inhibitors, CAR-T cell treatment, and cancer vaccines [10–12]. These therapies are actively being studied and developed because they have demonstrated encouraging outcomes in treating various cancer types [13]. However, the interconnection between ion channels and immunotherapy in PDAC has yet to be explored.

The prognostic biomarker genes TRPV2 and GJB3, which are based on the ion channel gene, were screened, and a novel prognostic model was created to accurately predict the prognosis of PDAC patients. TRPV2 and GJB3 were further found as potent cancer immunotherapy determinants.

2. Materials and methods

2.1. Data source

The Cancer Genome Atlas (TCGA) database extracted the transcriptome data of 172 pancreatic ductal adenocarcinoma (PDAC) tissues and 4 normal tissues with complete clinical information. The GSE78229 dataset's transcriptome data and complete clinical information were obtained from the Gene Expression Omnibus (GEO) database. The dataset GSE782229 contained 49 PDAC samples with survival data. The HUGO Gene Nomenclature Committee (HGNC) database provided the list of 328 ion channel genes.

2.2. Identification of differentially expressed ion channel genes (DEICGs)

The 'limma' R package was utilized to extract the differentially expressed ion channel genes (DEICGs) (P-value <0.05, $|\log2$ Fold Change (FC)$| > 0.5$) in the TCGA-PDAC dataset between normal and PDAC tissues [14,15].

2.3. Functional enrichment analysis

GO (BP, CC, MF) and KEGG enrichment analyses were implemented on the Metascape website, and the functions of DEICGs were annotated.

2.4. Construction and validation of the prognostic model

We randomly split 172 samples from the TCGA-PDAC dataset into 69 testing and 103 training sets, with a 6:4 ratio. DEICGs that were substantially (P-value <0.2) correlated with the OS of the PDAC patients in the training sample were found using the univariate Cox regression model [16]. The potential DEICGs were then put through a stepwise multivariate regression analysis to assess how well they predicted patient survival [17,18]. The formula used to calculate the risk score was: $\text{Riskscore} = \beta1X1 + \beta2X2 + \ldots + \beta nXn$. The gene expression level is represented by X1 in this formula, and the regression coefficient is denoted by β. Using the R software's "survminer" package, the median risk score was calculated to divide patients into high- and low-risk groups. The OS between two risk groups was then assessed using the K-M survival curve and the log-rank test. Using the R software's "survival ROC" package, the receiver operating characteristic (ROC)'s area under the curve (AUC) was determined. The R software's "pheatmap" package also depicted the risk plot. The GSE78229 dataset's patients (49 samples) served as the validation set, and the testing and validation sets underwent the same process to verify the risk model.

2.5. Independent prognostic analysis and construction of a nomogram

Using the TCGA-PDAC dataset, univariate and multivariate Cox regression analyses were used to find independent prognostic predictors. Next, using the R packages "rms" and "nomogramEx," a nomogram with the risk score and clinicopathological parameters was created. Using the R package "regplot," we created calibration curves (1, 3, and 5 years) to confirm the nomogram's correctness.

2.6. Gene set enrichment analysis

Using the R software's "clusterProfiler" package, KEGG-based GSEA was conducted to examine the various signaling pathways that separate the low- and high-risk groups in the TCGA-PDAC dataset [19,20].

2.7. Evaluation of immunotherapy efficiency

There was a comparison of immune checkpoint molecule expression in two risk groups. The Tumor Immune Dysfunction and Exclusion (TIDE) is a computational technique to predict possible responsiveness to cancer immunotherapy [21].

2.8. Verification of gene expression

The prognostic gene's protein expression was compared using the Human Protein Atlas (HPA) database.

2.9. Experimental validation

The SW1990 and THP-1 cell lines were purchased from iCell (Shanghai, China, http://www.icellbioscience.com/search) as previously described [22]. SiRNA sequences of TRPV2: Forward GCCGGATCCAAACCGATTTGA; Forward GCTGGAGATCATTGCCTTTCA; Forward GCTGGCTGAACCTGCTTTACT. Please see the supplementary materials for the detailed methods.

2.10. Statistical analysis

The R project was used for all analyses, and the Wilcoxon and Kruskal-Wallis tests were used to compare the data from various groups. P-values of less than 0.05 were deemed statistically significant in all analyses.

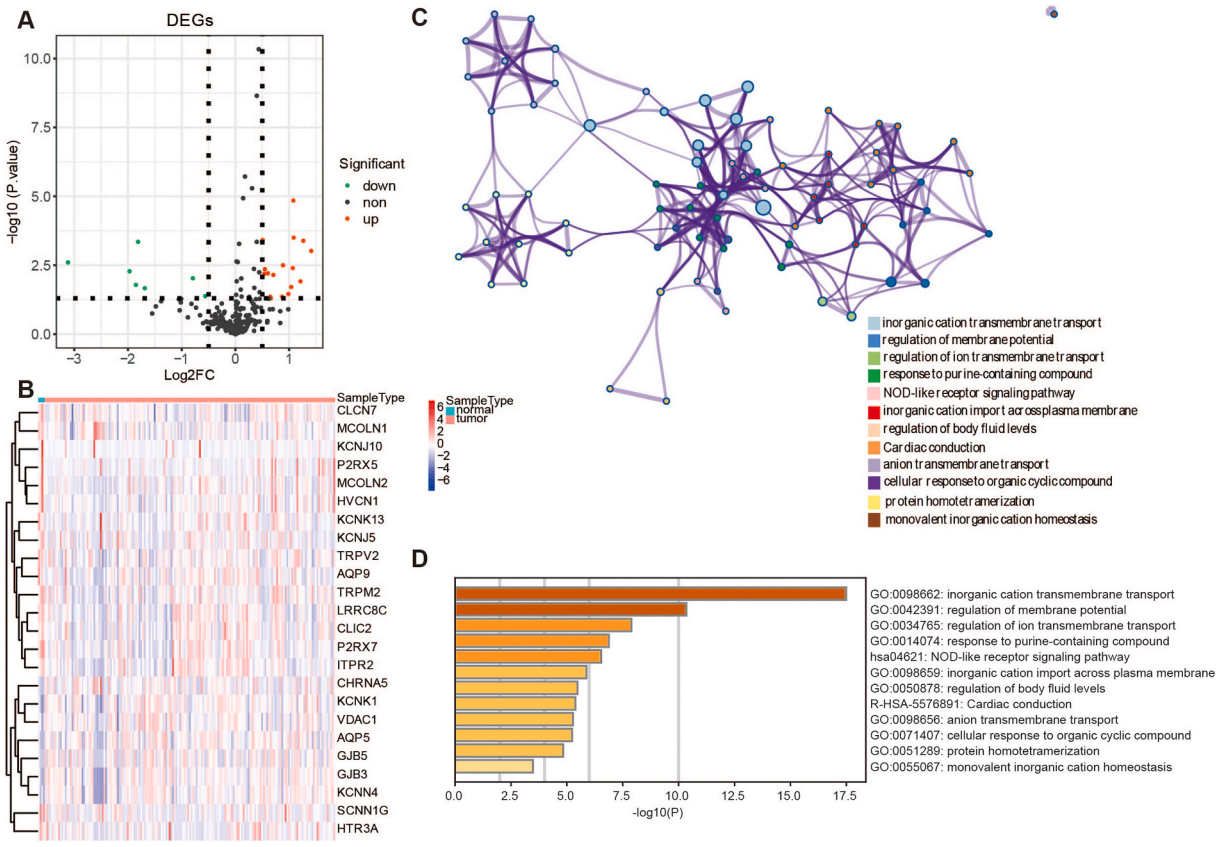

Fig. 1. Identification of DEICGs in PDAC. (A)Volcano plot of all DEICGs. The orange dot represents up-regulated genes, the green dot represents down-regulated genes, and the grey dot represents unchanged genes. DEICGs: differentially expressed ion channel genes. (B) Heat maps of DEICGs. Functional and pathway enrichment analysis of DEICGs. (C–D) Contains 10 GO terms and 2 KEGG pathways. (For interpretation of the references to colour in this figure legend, the reader is referred to the Web version of this article.)

3. Results

3.1. The DEICGs expression profile in PDAC

We delineated the expression pattern of 328 ion channel genes in normal and PDAC samples in the TCGA-PDAC dataset. 24 DEICGs, including 17 up-regulated and seven down-regulated genes, were screened and listed in Supplementary Table 1. The DEICGs expression profile was shown in a volcano map and a heatmap (Fig. 1A-B).

3.2. Functional enrichment based on DEICGs

Next, DEICGs were enriched in 10 GO pathways and 2 KEGG pathways (Fig. 1C-D). These DEICGs were mainly joined in some biological processes, such as membrane potential regulation and ion transmembrane transport, etc. Meanwhile, these DEICGs were enriched in NOD-like receptor signaling and cardiac conduction pathways.

3.3. Construction and internal validation of the ICGs-related prognostic risk model

Two datasets comprising 103 cases for training and 65 patients for testing were created from the 172 PDAC patients. Next, utilizing 24 DEICGs from the training group, a univariate Cox regression analysis was conducted to identify prognoses-related genes. In the training set, 10 of the 24 DEICGs were found to be strongly correlated with patients' overall survival (P-value < 0.2) (Table 1). A stepwise multivariate Cox regression analysis was performed on the 10 DEICGs. As predictive genes, two DEICGs (TRPV2 and GJB3) were found (Fig. 2A), along with each regression coefficient. To assess patients' prognoses more accurately, we created a prognostic risk model as "0.2874 $\times$ expression of GJB3 and 0.4332 $\times$ expression of TRPV2". Based on the median value of the risk score in the training and testing sets, the patients were categorized into two risk groups to evaluate the availability of the prognostic model. A K-M survival analysis was then carried out. The findings revealed that compared to low-risk scores, those with high-risk scores had noticeably worse survival rates (Fig. 2B, F). In the training set, the 1-, 3-, and 5-year OS AUC values were 0.627, 0.785, and 0.717, respectively, showing a respectable accuracy (Fig. 2C). Concurrently, the testing set's 1-, 3-, and 5-year OS AUC values were 0.622, 0.749, and 0.751, respectively, indicating a robust predictive ability for the risk score (Fig. 2G). Fig. 2D, E, 2H, and 2I showed the TRPV2 and GJB3 expression heatmap in the training set and testing set. The heatmap data indicated the high-risk group had high expression levels of the dangerous ICGs, TRPV2 and GJB3. Besides, with increasing risk ratings, patients faced more significant mortality risks, according to the survival status distribution map.

3.4. External validation of the ICGs-related prognostic risk model

To test the model accuracy externally, we employed a cohort of 49 PDAC patients from the GEO dataset GSE78229, which is independent. In the validation set, high-risk patients showed worse OS (Fig. 3A), consistent with the TCGA cohorts. As a result, according to Fig. 3B, the 1-year AUC value is 0.647, and the 3-year AUC value is 0.678. Fig. 3C-D displayed the survival status based on patients

Table 1
Univariate Cox regression analysis.

Gene	HR	HR.95L	HR.95H	Cox P value
GJB3	1.33729	1.05171	1.700417	0.0177253
MCOLN1	0.442868	0.219608	0.893098	0.0228532
TRPV2	1.601132	1.044604	2.454158	0.0307548
KCNN4	1.183696	0.984241	1.423569	0.0732539
AQP5	1.130664	0.979798	1.30476	0.0928283
AQP9	1.248074	0.915524	1.701419	0.1610051
CLCN7	0.533481	0.2204	1.291298	0.1635774
KCNK13	1.824279	0.765605	4.346882	0.1747619
KCNK1	1.220253	0.912706	1.631432	0.1791161
GJB5	1.15223	0.933102	1.422817	0.1879703
VDAC1	1.235671	0.708988	2.15361	0.4553085
CHRNA5	1.207642	0.72556	2.010032	0.4679565
CLIC2	1.122822	0.77271	1.631569	0.5434631
P2RX5	0.881997	0.582236	1.336089	0.5534626
SCNN1G	0.893119	0.608602	1.310646	0.5635286
KCNJ10	0.686698	0.151924	3.103885	0.625307
TRPM2	1.112963	0.703615	1.760461	0.6473432
LRRC8C	1.1428	0.643916	2.028203	0.6483565
MCOLN2	0.896982	0.526288	1.528777	0.6894178
HTR3A	1.066684	0.733008	1.552255	0.7359182
P2RX7	1.070384	0.625848	1.830672	0.8038198
KCNJ5	1.03124	0.735115	1.446653	0.8586267
HVCN1	0.984177	0.642483	1.507596	0.9415668
ITPR2	1.011512	0.712792	1.43542	0.9488938

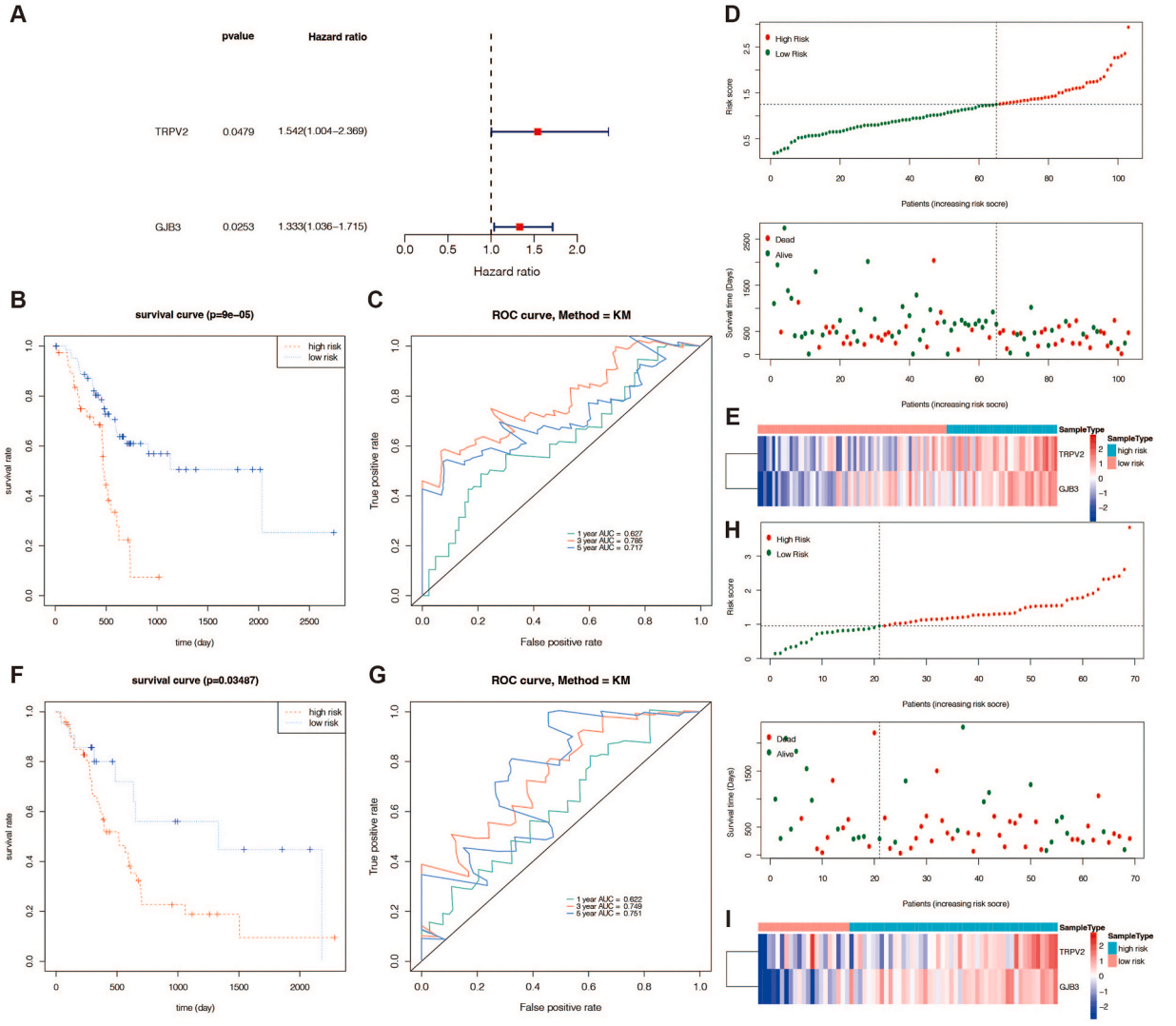

Fig. 2. Construction and internal validation of the ICGs-related prognostic risk model. (A) The multivariate Cox regression analysis. TRPV2: p-value = 0.0479. GJB3: p-value = 0.0253. (B) The survival curves of the training set and the testing set were, respectively, high-risk group and low-risk group. The training set: p = 9e-05. (C) ROC curve of the training set AUC. The green line represents 1 year AUC, the orange line represents 3-year AUC, and the blue line represents 5-year AUC. 1 year AUC = 0.627, 3 years AUC = 0.785, 5 years AUC = 0.717. (D) The distribution of ranked risk scores and survival status of individual patients. (E) The heatmap of 2 prognostic genes expression in the training set. (F) The survival curves of the training set and the testing set were, respectively, high-risk group and low-risk group. The testing set: p = 0.03487. (G) ROC curve of the testing set AUC. 1 year AUC = 0.622, 3 year AUC = 0.749, 5 year AUC = 0.751. (H) The distribution of ranked risk scores and survival status of individual patients. (I) The heatmap of 2 prognostic genes expression in the testing set. (For interpretation of the references to colour in this figure legend, the reader is referred to the Web version of this article.)

with higher risk scores. The heatmap result indicated that TRPV2 and GJB3 were more expressed in the high-risk group. These findings further supported the accuracy of the ICGs-related risk model in predicting PDAC patients' 1- and 3-year overall survival.

3.5. Independent prognostic of the risk model and nomogram construction

The risk score was then tested for independence from other clinical factors (age, gender, and stage) as a prognostic factor for PDAC patients using univariate and multivariate Cox regression analysis. The results of the univariate analysis showed that age and risk score were prognostic indicators (Fig. 3E). The risk score can be utilized independently to forecast a patient's prognosis (Fig. 3F). Furthermore, the multivariate analysis revealed that age was a significant predictive factor as well. Then, using age and risk score, we created a nomogram to predict patients' 1-, 3-, and 5-year OS (Fig. 3G). According to the calibration plots, the nomogram did an excellent job projecting the 1-, 3-, and 5-year survival probabilities for PDAC patients (Fig. 3H).

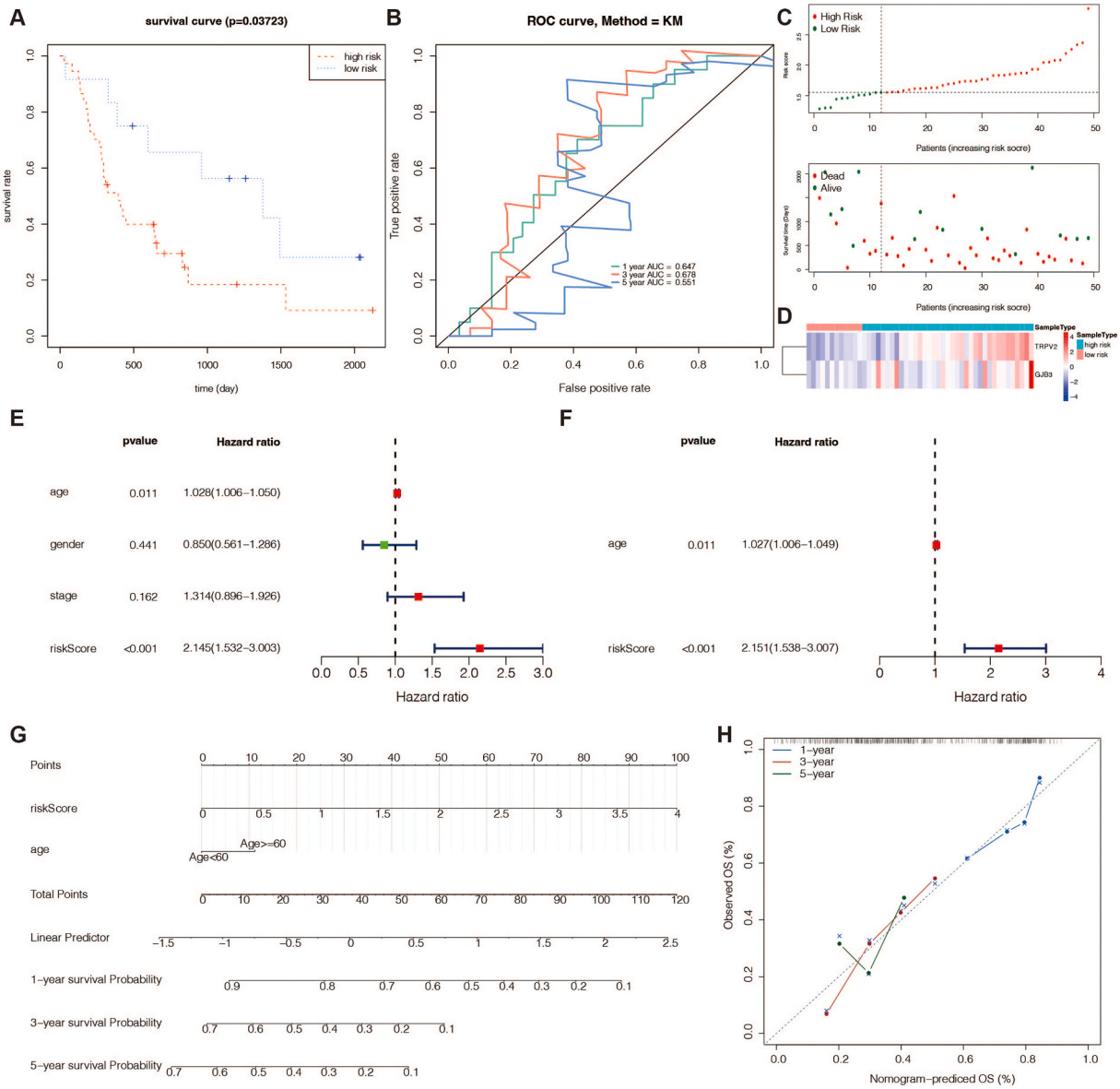

Fig. 3. Validation of the ICGs-related prognostic risk model via external cohort (A) The survival curves of high-risk group and low-risk group from GEO datasets. (B) ROC curve of the GEO datasets AUC. 1 year AUC = 0.647, 3 year AUC = 0.678, 5 year AUC = 0.551. (C) The survival status based on patients with increased risk scores. (D) The heatmap of the TRPV2 and GJB3 in the high-risk group. Independent prognostic of the risk model and nomogram construction (E) The univariate analysis. Age: p = 0.011. Risk score : <0.001. (F) The multivariate Cox regression analyses. Age: p = 0.011. Risk score : <0.001.(G) Using age and risk scores, a nomogram is constructed to predict patients' OS for 1-, 3-, and 5 years. (H) The calibration plots. The blue line represents 1 year AUC, The red line represents 3 year AUC, The green line represents 5 year. (For interpretation of the references to colour in this figure legend, the reader is referred to the Web version of this article.)

3.6. GSEA for the two risk groups

To investigate potential mechanisms underlying the prognostic gap, GSEA was utilized to examine the route enrichment between the high-risk and low-risk groups. The top eight significant pathways are shown in Fig. 4A. Notably, these pathways, including influenza A, microRNAs in cancer, NOD-like receptor signaling pathway, osteoclast differentiation, PI3K-AKT signaling pathway, proteoglycans in cancer, and staphylococcus aureus infection were more active in the high-risk group as ES values > 0.

3.7. Evaluation of immunotherapy efficiency between the two risk groups

Immune checkpoint molecules offer a variety of therapeutic applications in immunotherapy and are necessary for immune function

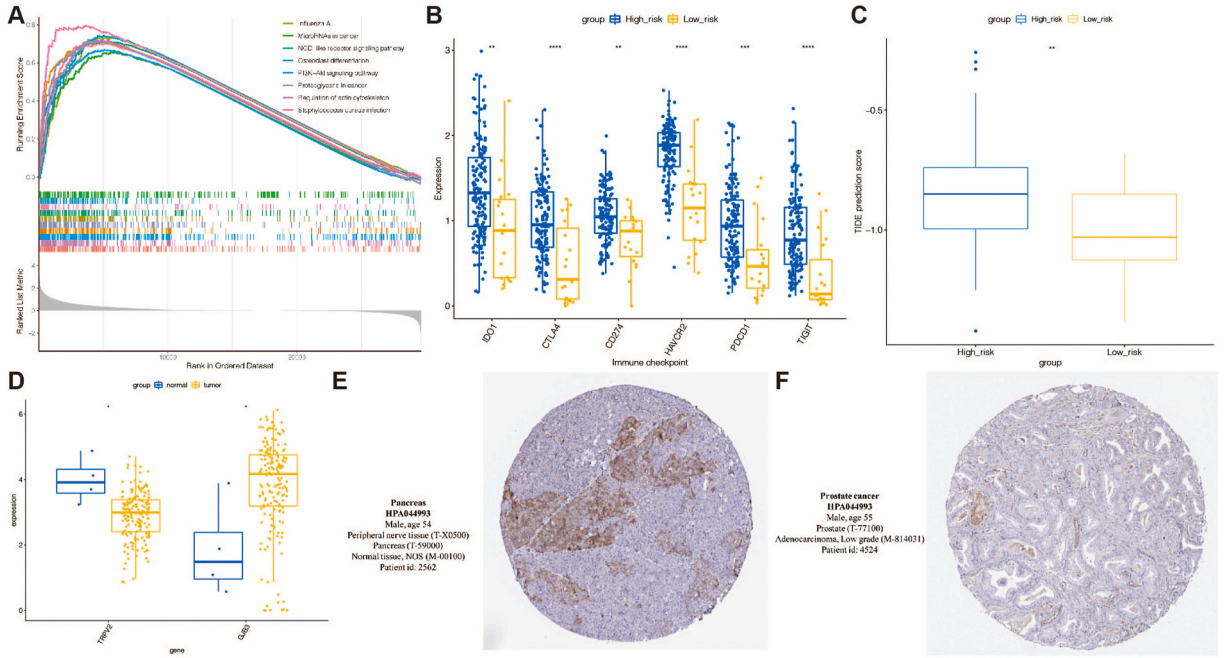

Fig. 4. Functional annotation of the risk groups. GSEA between the high-risk and low-risk groups. Evaluation of immunotherapy efficiency between the two risk groups (A) Differential expression of immune checkpoints. Blue group represent high-risk, Yellow group represent low-risk. (B) The TIDE score of the two risk groups. The expression of prognostic genes in the HPA Database (A) Expression of biomarkers in tumor and normal tissues. Blue group represent normal tissue, Yellow group represent tumor tissue. (B) Immunohistochemistry in the HPA database. (For interpretation of the references to colour in this figure legend, the reader is referred to the Web version of this article.)

[23]. Firstly, we explored the expression pattern of IDO1, CTLA4, PD-L1(CD274), HAVCR2, PD-1(PDCD1), and TIGIT in low- and high-risk groups. As shown in Fig. 4B, these immune checkpoint molecules were up-regulated in the high-risk group, promoting the development of PDAC. Then, we calculated and compared the TIDE scores in two risk groups. As revealed in Fig. 4C, the TIDE score of the high-risk group was higher than the low-risk group, indicating that ICB therapy in the high-risk group was poorly effective.

3.8. Verification of prognostic genes in the HPA database

As demonstrated in Fig. 4D, GJB3 was up-regulated in PDAC samples, while TRPV2 was down-regulated at the transcriptional level compared to normal samples. The HPA database was searched for associated gene immunohistochemistry results from normal and malignant tissues to confirm the expression of TRPV2 and GJB3 at the protein level. The transcriptional level was consistent with the outcome, demonstrating a significant decrease in TRPV2 protein expression in PDAC (Fig. 4E). Nonetheless, the HPA database did not have information on GJB3's protein expression.

3.9. Functional annotation of TRPV2 and GJB3

As shown in Fig. S1A, cellular component organization, cell periphery, and molecular function were related to GJB3. As shown in Fig. S1B, leukocyte activation, cell periphery, and molecular transducer activity were related to TRPV2.

3.10. Immune infiltration characteristics of TRPV2 and GJB3

As shown in Fig. S2A, M0/M1 macrophages, Th1 cells, Tgd cells, iDC, Tregs, and resting NK cells were positively related to GJB3. As shown in Fig. S2B, DCs, neutrophils, macrophages, fibroblasts, CD4/CD8 T cells, and M1/M2 macrophages were positively related to TRPV2.

3.11. Drug prediction on TRPV2 and GJB3

As shown in Fig. 5, the drug prediction on TRPV2 (Fig. 5A-D) and GJB3 (Fig. 5E-H) was performed in GDSC1, GDSC2, CTRP, and PRISM databases. Patients with PAAD who exhibit high levels of TRPV2 are susceptible to some medications, including fumonisin B1, JAK3_7406_1434, Refametinib_1526, and selumetinib: PLX-4032. Furthermore, medications like ERK_2440_1713, flibanserin, sapitinib_1549, and PD-102807 are sensitive to patients with PAAD who have high GJB3 expression.

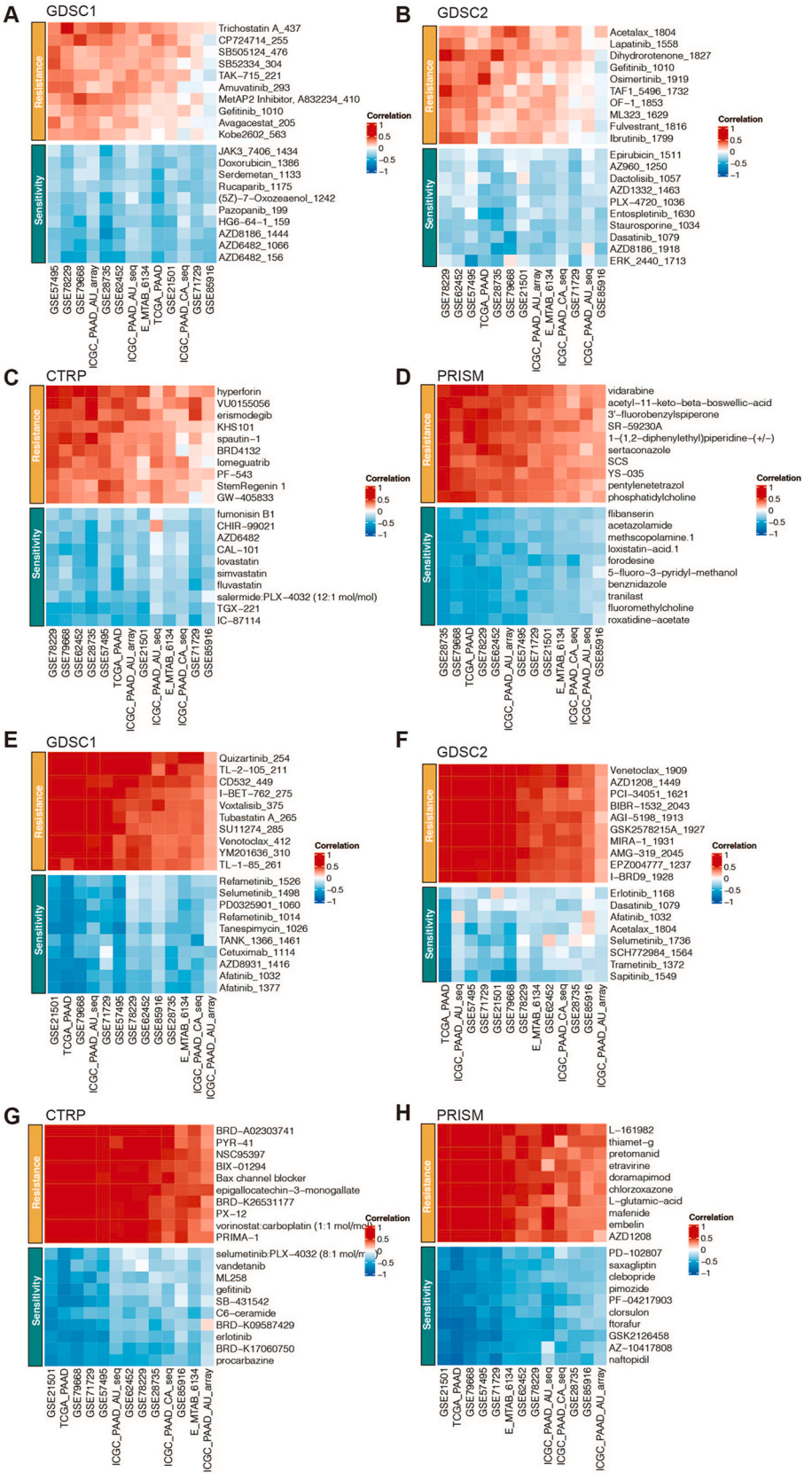

(caption on next page)

Fig. 5. Drug prediction on TRPV2 and GJB3. The drug prediction on TRPV2 and GJB3 was performed in GDSC1, GDSC2, CTRP, and PRISM databases.

3.12. Immunotherapy prediction on TRPV2 and GJB3

As shown in Fig. S2C, NT5E, CD276, TNFSF9, CCL20, CCL13, CXCL8, IL10RB, LGALS9, and TGFB1 were positively related to GJB3. As shown in Fig. S2D, CCL18, CCL5, CCL13, HAVCR2, CSF1R, TIGIT, TNFSF4, CD80, and IL2RA were positively related to TRPV2. As shown in Fig. 6, TRPV2 could predict immunotherapy response in Hugo, Homet, Cho, and VanAllen cohorts (Fig. 6A). TRPV2 was associated with significantly worse survival in Cho and Nathanson cohorts (Fig. 6B). Besides, GJB3 could predict immunotherapy response in Lausss, Homet, Gao, Amato, Wolf, and Nathanson cohorts (Fig. 6C).

3.13. Mutation characteristics of TRPV2 and GJB3

As shown in Fig. 7, TRPV2 could predict a gain of 12p13.33, 12p11.21, 12q15, and 17q12 while a loss of 1p36.11. Besides, GJB3 could predict a loss of 17p12, 17q22, 19p13.3, and 19p13.2.

3.14. In vitro validation on TRPV2

qPCR assay was conducted for optimal siRNA targets (Fig. 8A). CCK8 assay for TRPV2 showed that PDAC cells in two siRNA groups had inhibited proliferation ability (Fig. 8B). EdU assay for TRPV2 showed that PDAC cells in two siRNA groups had inhibited proliferation ability (Fig. 8C-D). Transwell assay for TRPV2 showed that PDAC cells in two siRNA groups had inhibited migration ability (Fig. 8E-F). The co-culture Transwell assay for TRPV2 showed that macrophages in two siRNA groups had inhibited migration ability (Fig. 8G-H).

4. Discussion

One of the most deadly tumors in the world, pancreatic ductal adenocarcinoma (PDAC), still has no proven treatment. The leading causes of PDAC's poor overall prognosis are early distant metastases, delayed diagnosis, and inadequate treatment plans [24]. Ion channels are essential to the development of cancer and are involved in numerous physiological processes. Ion channel genes are involved with pancreatic cancer in earlier research.

This study used mRNA expression data and 328 ion channel genes between normal and PDAC samples in the TCGA-PDAC dataset to analyze genes associated with PDAC prognosis. Functional enrichment informed that these DEICGs were mainly joined in membrane potential regulation, ion transmembrane transport, etc. Meanwhile, these DEICGs were enriched in the NOD-like receptor signaling and cardiac conduction pathways. Zhao et al. [25] revealed that Artesunate induces apoptosis of lung cancer cells by decreasing mitochondrial membrane potential dose-dependently. Using bis (thiourea) derivatives of 1, 2-phenylenediamine scaffolds, Nasim and colleagues synthesized Cl— ion transporters. They discovered that Cl— transport activity was inversely proportional to IC50 values of various cancer cell lines, indicating that Cl— ion activity can affect cancer cell apoptosis. Hao Yang et al. [26] prepared a compound with hepatocellular carcinoma cell targeting by adding galactose gA peptide to the N-terminal. The conjugates form monomolecular transmembrane channels on the cell membrane, which can transport monovalent cations and induce apoptosis of cancer cells.

Then, combined with clinical survival information, TRPV2 and GJB3 were revealed as potential prognostic markers associated with patient survival. TRPV2 reportedly mediates cell survival, proliferation, and metastasis [27]. TRPV2 with altered expression profile showed oncogenic ability in leukemia and bladder cancer [28]. In patients with multiple myeloma, TRPV2 was associated with bone tissue damage and led to poor prognosis [29]. In prostate cancer, TRPV2 was linked to resistance to castration and tumor metastasis [30]. Some research has reported a significant correlation between GJB3 and survival rate in breast cancer patients with bone metastasis. GJB3 was a potential marker or molecular target for melanoma [31]. These results imply that GJB3 and TRPV2 primarily function as oncogenes, accelerating the growth of tumors. Similarly, our findings also demonstrated that GJB3 was up-regulated in PDAC samples while TRPV2 was down-regulated at the transcriptional level compared to normal samples. Regretfully, more research is needed to determine its precise process.

We developed a predictive risk model to assess patient prognosis more accurately since we discovered TRPV2 and GJB3 as promising prognostic markers. As confirmed by internal and external cohorts, the results indicated that patients with low-risk scores had much higher survival rates than those with high-risk scores. TRPV2 and GJB3 were also strongly expressed in high-risk groups and were linked to a bad prognosis. After confirming that the risk score was unrelated to age, gender, and stage, among other clinical factors, multivariate Cox regression analysis revealed that risk scores may be used independently to predict PDAC patients' prognosis. Additionally, we created a nomogram to forecast the chance of 1-, 3-, and 5-year survival for patients with PDAC.

Besides, TRPV2 and GJB3 may be involved in developing patients' diseases and affect their prognosis by participating in microRNAs in cancer, NOD-like receptor signaling pathway, osteoclast differentiation, P13K-AKT signaling pathway, and proteoglycans in cancer, as illustrated in the results section. A systematic expression analysis of 217 mammalian miRNAs from 334 samples—including several human cancers—was disclosed by Lu et al. They discovered that malignancies generally have lower levels of miRNAs than normal tissues [32]. Subsequent studies have also confirmed that reduced miRNA can lead to tumorigenesis in most cases. Still, some miRNA upregulation can lead to the occurrence of cancer, including miR-21 [33], miR-155 and miR-17~19b [34], and miR-106b-5p

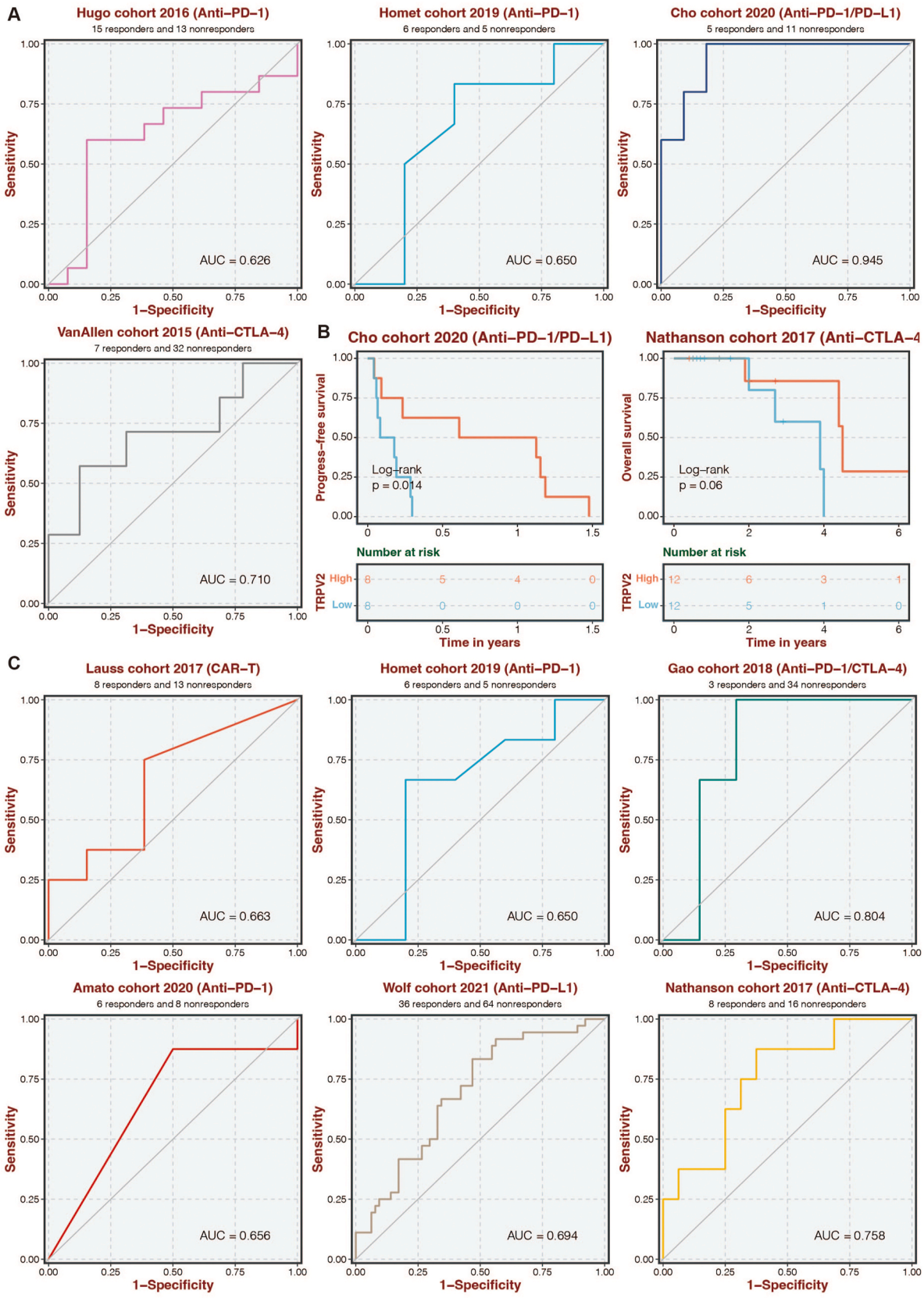

(caption on next page)

Fig. 6. Immunotherapy prediction on TRPV2 and GJB3. Immunotherapy response predictions of TRPV2 in Hugo, Homet, Cho, and VanAllen cohorts. The survival curves of TRPV2-based groups in Cho and Nathanson cohorts. The survival curves of GJB3-based groups in Lausss, Homet, Gao, Amato, Wolf, and Nathanson cohorts.

[35]. Hu et al. reported that PC cells and tissues have significant levels of NLRP3 expression. Knocking down NLRP3 can inhibit cell proliferation and invasion, reverse EMT, increase e-CAD, and reduce Vimentin, suggesting that NLRP3 may play an essential role in tumor progression [36]. Xu et al. [37] found that the PI3K/Akt/mTOR signaling pathway may have a role in treating pancreatic cancer. Li et al. [38] showed that PI3K/Akt signaling pathway contributed to tumor progression of pancreatic cancer.

Pancreatic cancer, one of the most deadly and aggressive solid malignancies, is characterized by subtle clinical symptoms, a quick course, a dismal prognosis, and a high death rate. The five-year survival rate for PDAC is as low as 9%, even with advancements in surgical skills, chemotherapy regimens, and the advent of neoadjuvant chemoradiotherapy. Furthermore, immunotherapy has recently gained a lot of attention as the hottest cancer treatment option. However, the majority of patients do not benefit. Thus, tailored therapy for patients with HNSCC may be possible through the identification of valuable markers that aid in predicting a patient's response to treatment. The expression of immune checkpoint molecules in the high-risk groups, such as IDO1, CTLA4, PD-L1(CD274), HAVCR2, PD-1(PDCD1), and TIGIT, was shown to be up-regulated in the TRPV2/GJB3-based prognostic model. This accelerated tumor development and had an impact on prognosis. Immunotherapy has made significant progress in recent years and has become a promising treatment option for various diseases, including cancer. Immunotherapy has shown great potential in improving patient outcomes and has sometimes led to long-lasting remissions. It is an exciting field of research and continues to evolve with discoveries and advancements [39]. PD-1/PD-L1 ICB can reverse the immunosuppressive microenvironment in patients, thereby significantly improving prognosis [40]. In the context of immunotherapy, ion channels have been found to have potential connections. For example, specific ion channels have been implicated in regulating immune cell activation and migration. Modulating the activity of these ion channels may enhance the effectiveness of immunotherapy treatments. One specific example is the role of potassium channels in T-cell activation. T cells are crucial in the immune response. It has been demonstrated that potassium channels govern T-cell activation via influencing these cells' membrane potential and calcium signaling. Modulating the activity of potassium channels could enhance T-cell activation and improve the efficacy of immunotherapy [41]. We calculated that the high-risk group had a higher TIDE score, indicating that it was less effective at receiving ICBs. Therefore, we speculate that TRPV2 and GJB3 can be used as molecular targets for potential immunotherapy. Notably, our findings further proved this speculation. TRPV2 and GJB3 were related to the expression levels of multiple immune checkpoints. Besides, TRPV2 and GJB3 could predict immunotherapy responses in multiple immunotherapy cohorts.

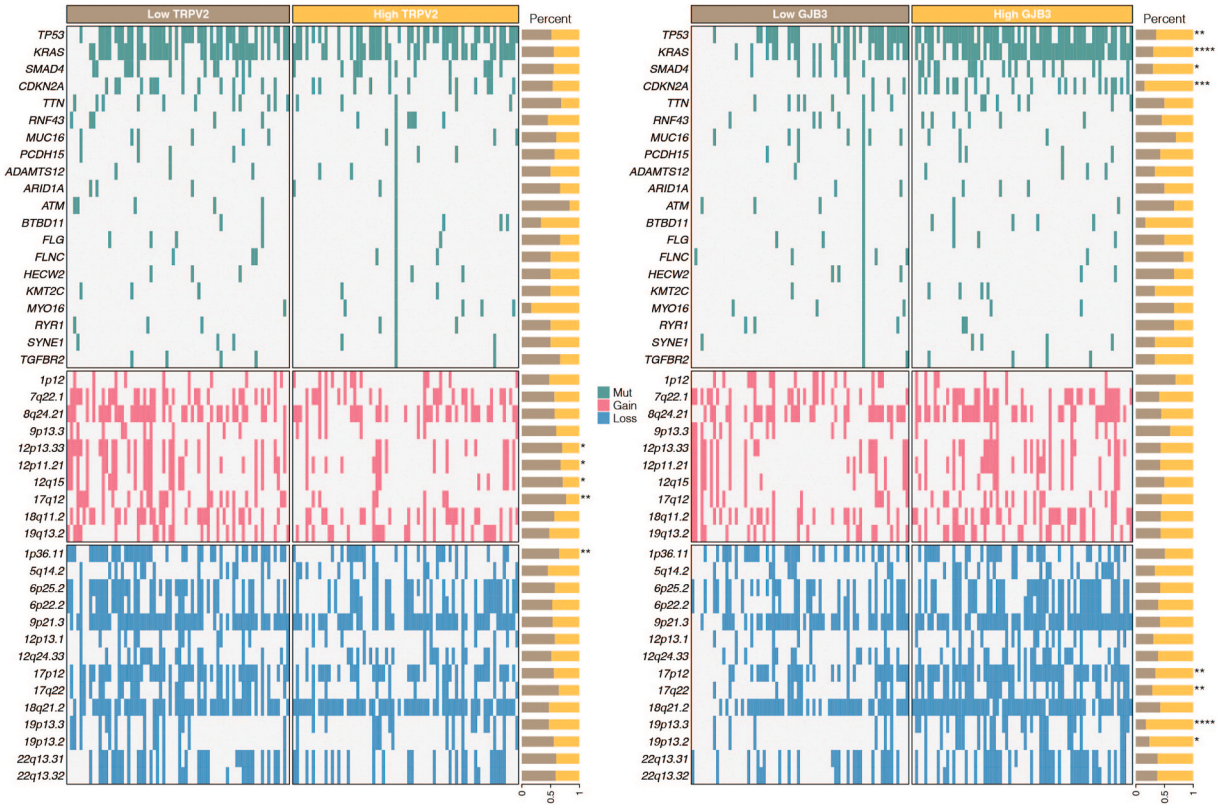

Fig. 7. Mutation characteristics of TRPV2 and GJB3.

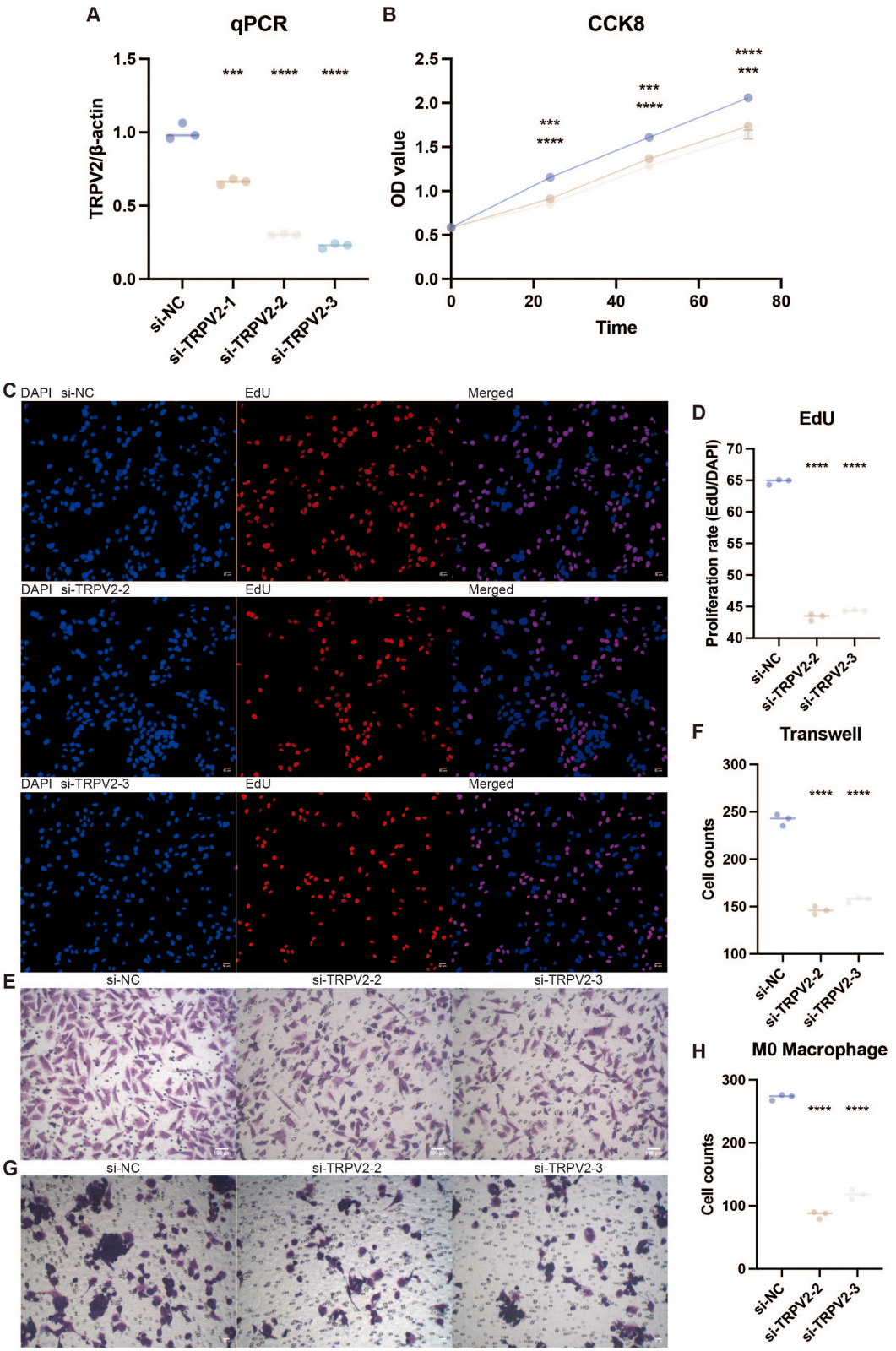

Fig. 8. Experimental validation on TRPV2. A. qPCR assay for optimal siRNA targets. B. CCK8 assay for TRPV2. C. EdU assay for TRPV2. D. Statistical analysis of EdU assay for TRPV2. E. Transwell assay for TRPV2. F. Statistical analysis of Transwell assay for TRPV2. G. Co-culture Transwell assay for TRPV2. H. Statistical analysis of Co-culture Transwell assay for TRPV2.

TRPV2 has been found to regulate immune cell activation and migration, and its expression has been associated with the efficacy of immunotherapies such as checkpoint inhibitors [42]. GJB3 is involved in the activation and proliferation of T cells. It has also been found to regulate immune cell infiltration into tumors [43].

Our in vitro validation laid a solid foundation for the tumor-promotive role of TRPV2. TRPV2 may encourage PDAC migration and multiplication. In addition, TRPV2 could promote the recruitment of macrophages. It is possible that TRPV2 may interact with other molecules or signaling pathways involved in macrophage activation or function.

5. Conclusion

In summary, we have discovered for the first time the ion channel genes TRPV2 and GJB3 linked to the prognosis of PDAC in this investigation. We created the nomogram and the related risk model. Further research and clinical validation are necessary to validate our conclusion fully. To be more precise, an outside group is required to verify the model and the ion channel genes TRPV2 and GJB3. Furthermore, future in vitro and in vivo studies will examine the precise processes by which the ion channel genes TRPV2 and GJB3 impact immunotherapy. Consequently, we will keep an eye on these genes' future functions.

Ethics statement

Not Applicable.

Funding

Natural Science Foundation of Liaoning Province (Grant No. 2021-BS-204).

Data availability statement

The datasets analyzed during the current study are available in the Gene Expression Omnibus (https://www.ncbi.nlm.nih.gov/geo/) and TCGA data source (https://xena.ucsc.edu).

CRediT authorship contribution statement

Jiakai Mao: Writing – original draft, Validation, Methodology, Investigation, Formal analysis, Data curation, Conceptualization. **Yu Tian:** Writing – original draft, Validation, Methodology, Investigation, Formal analysis, Data curation, Conceptualization. **Nan Luo:** Writing – review & editing, Validation, Supervision, Formal analysis, Data curation, Conceptualization.

Declaration of competing interest

The authors declare that they have no known competing financial interests or personal relationships that could have appeared to influence the work reported in this paper.

Acknowledgments

None.

Appendix A. Supplementary data

Supplementary data to this article can be found online at https://doi.org/10.1016/j.heliyon.2024.e27301.

References

[1] C.J. Halbrook, C.A. Lyssiotis, M. Pasca di Magliano, A. Maitra, Pancreatic cancer: advances and challenges, Cell 186 (8) (2023) 1729–1754, https://doi.org/10.1016/j.cell.2023.02.014.

[2] K. Saotome, S.E. Murthy, J.M. Kefauver, T. Whitwam, A. Patapoutian, A.B. Ward, Structure of the mechanically activated ion channel Piezo1, Nature 554 (7693) (2018) 481–486, https://doi.org/10.1038/nature25453.

[3] N. Prevarskaya, R. Skryma, Y. Shuba, Ion channels in cancer: are cancer hallmarks oncochannelopathies? Physiol. Rev. 98 (2) (2018) 559–621, https://doi.org/10.1152/physrev.00044.2016.

[4] G. Santoni, F. Maggi, M.B. Morelli, M. Santoni, O. Marinelli, Transient receptor potential cation channels in cancer therapy, Med. Sci. 7 (12) (2019), https://doi.org/10.3390/medsci7120108.

[5] R. Rao, S. Shah, D. Bhattacharya, D.K. Toukam, R. Caceres, D.A. Pomeranz Krummel, S. Sengupta, Ligand-gated ion channels as targets for treatment and management of cancers, Front. Physiol. 13 (2022) 839437, https://doi.org/10.3389/fphys.2022.839437.

[6] Z.D. Hu, J. Yan, K.Y. Cao, Z.Q. Yin, W.W. Xin, M.F. Zhang, MCOLN1 promotes proliferation and predicts poor survival of patients with pancreatic ductal adenocarcinoma, Dis. Markers (2019) 9436047, https://doi.org/10.1155/2019/9436047, 2019.

[7] R. Lin, Y. Wang, Q. Chen, Z. Liu, S. Xiao, B. Wang, B. Shi, TRPM2 promotes the proliferation and invasion of pancreatic ductal adenocarcinoma, Mol. Med. Rep. 17 (6) (2018) 7537–7544, https://doi.org/10.3892/mmr.2018.8816.

[8] C.S. Yiong, T.P. Lin, V.Y. Lim, T.B. Toh, V.S. Yang, Biomarkers for immune checkpoint inhibition in sarcomas - are we close to clinical implementation? Biomark. Res. 11 (1) (2023) 75, https://doi.org/10.1186/s40364-023-00513-5.

[9] Q. Dong, T. Xue, H. Yan, F. Liu, R. Liu, K. Zhang, Y. Chong, J. Du, H. Zhang, Radiotherapy combined with nano-biomaterials for cancer radio-immunotherapy, J. Nanobiotechnol. 21 (1) (2023) 395, https://doi.org/10.1186/s12951-023-02152-2.

[10] Z. Pang, M.M. Lu, Y. Zhang, Y. Gao, J.J. Bai, J.Y. Gu, L. Xie, W.Z. Wu, Neoantigen-targeted TCR-engineered T cell immunotherapy: current advances and challenges, Biomark. Res. 11 (1) (2023) 104, https://doi.org/10.1186/s40364-023-00534-0.

[11] K. Pang, Z.D. Shi, L.Y. Wei, Y. Dong, Y.Y. Ma, W. Wang, G.Y. Wang, M.Y. Cao, J.J. Dong, Y.A. Chen, P. Zhang, L. Hao, H. Xu, D. Pan, Z.S. Chen, C.H. Han, Research progress of therapeutic effects and drug resistance of immunotherapy based on PD-1/PD-L1 blockade, Drug Resist. Updates 66 (2023) 100907, https://doi.org/10.1016/j.drup.2022.100907.

[12] A. He, X. Li, Z. Dai, Q. Li, Y. Zhang, M. Ding, Z.F. Wen, Y. Mou, H. Dong, Nanovaccine-based strategies for lymph node targeted delivery and imaging in tumor immunotherapy, J. Nanobiotechnol. 21 (1) (2023) 236, https://doi.org/10.1186/s12951-023-01989-x.

[13] J. Fan, K.K.W. To, Z.S. Chen, L. Fu, ABC transporters affects tumor immune microenvironment to regulate cancer immunotherapy and multidrug resistance, Drug Resist. Updates 66 (2023) 100905, https://doi.org/10.1016/j.drup.2022.100905.

[14] M.E. Ritchie, B. Phipson, D. Wu, Y. Hu, C.W. Law, W. Shi, G.K. Smyth, Limma powers differential expression analyses for RNA-sequencing and microarray studies, Nucleic Acids Res. 43 (7) (2015) e47, https://doi.org/10.1093/nar/gkv007.

[15] B. Phipson, S. Lee, I.J. Majewski, W.S. Alexander, G.K. Smyth, Robust hyperparameter estimation protects against hypervariable genes and improves power to detect differential expression, Ann. Appl. Stat. 10 (2) (2016) 946–963, https://doi.org/10.1214/16-AOAS920.

[16] S.J. Kang, Y.R. Cho, G.M. Park, J.M. Ahn, S.B. Han, J.Y. Lee, W.J. Kim, D.W. Park, S.W. Lee, Y.H. Kim, C.W. Lee, S.W. Park, G.S. Mintz, S.J. Park, Predictors for functionally significant in-stent restenosis: an integrated analysis using coronary angiography, IVUS, and myocardial perfusion imaging, JACC Cardiovasc Imaging 6 (11) (2013) 1183–1190, https://doi.org/10.1016/j.jcmg.2013.09.006.

[17] N. Simon, J. Friedman, T. Hastie, R. Tibshirani, Regularization paths for cox's proportional hazards model via coordinate descent, J. Stat. Software 39 (5) (2011) 1–13, https://doi.org/10.18637/jss.v039.i05.

[18] R. Tibshirani, The lasso method for variable selection in the Cox model, Stat. Med. 16 (4) (1997) 385–395, https://doi.org/10.1002/(sici)1097-0258(19970228)16:4<385::aid-sim380>3.0.co;2-3.

[19] A. Subramanian, P. Tamayo, V.K. Mootha, S. Mukherjee, B.L. Ebert, M.A. Gillette, A. Paulovich, S.L. Pomeroy, T.R. Golub, E.S. Lander, J.P. Mesirov, Gene set enrichment analysis: a knowledge-based approach for interpreting genome-wide expression profiles, Proc. Natl. Acad. Sci. U. S. A. 102 (43) (2005) 15545–15550, https://doi.org/10.1073/pnas.0506580102.

[20] V.K. Mootha, C.M. Lindgren, K.F. Eriksson, A. Subramanian, S. Sihag, J. Lehar, P. Puigserver, E. Carlsson, M. Ridderstrale, E. Laurila, N. Houstis, M.J. Daly, N. Patterson, J.P. Mesirov, T.R. Golub, P. Tamayo, B. Spiegelman, E.S. Lander, J.N. Hirschhorn, D. Altshuler, L.C. Groop, PGC-1alpha-responsive genes involved in oxidative phosphorylation are coordinately downregulated in human diabetes, Nat. Genet. 34 (3) (2003) 267–273, https://doi.org/10.1038/ng1180.

[21] J. Fu, K. Li, W. Zhang, C. Wan, J. Zhang, P. Jiang, X.S. Liu, Large-scale public data reuse to model immunotherapy response and resistance, Genome Med. 12 (1) (2020) 21, https://doi.org/10.1186/s13073-020-0721-z.

[22] S. Shao, Y. Sun, D. Zhao, Y. Tian, Y. Yang, N. Luo, A ubiquitination-related risk model for predicting the prognosis and immunotherapy response of gastric adenocarcinoma patients, PeerJ 12 (2024) e16868, https://doi.org/10.7717/peerj.16868.

[23] S. Singh, D. Hassan, H.M. Aldawsari, N. Molugulu, R. Shukla, P. Kesharwani, Immune checkpoint inhibitors: a promising anticancer therapy, Drug Discov. Today 25 (1) (2020) 223–229, https://doi.org/10.1016/j.drudis.2019.11.003.

[24] J. Dhillon, M. Betancourt, Pancreatic ductal adenocarcinoma, Monogr. Clin. Cytol. 26 (2020) 74–91, https://doi.org/10.1159/000455736.

[25] Y. Zhao, J. Liu, L. Liu, Artesunate inhibits lung cancer cells via regulation of mitochondrial membrane potential and induction of apoptosis, Mol. Med. Rep. 22 (4) (2020) 3017–3022, https://doi.org/10.3892/mmr.2020.11341.

[26] H. Yang, J. Wang, J.H. Fan, Y.Q. Zhang, J.X. Zhao, X.J. Dai, Q. Liu, Y.J. Shen, C. Liu, W.D. Sun, Y. Sun, Ilexgenin A exerts anti-inflammation and anti-angiogenesis effects through inhibition of STAT3 and PI3K pathways and exhibits synergistic effects with Sorafenib on hepatoma growth, Toxicol. Appl. Pharmacol. 315 (2017) 90–101, https://doi.org/10.1016/j.taap.2016.12.008.

[27] K.S. Siveen, P.B. Nizamuddin, S. Uddin, M. Al-Thani, M.P. Frenneaux, I.A. Janahi, M. Steinhoff, F. Azizi, TRPV2: a cancer biomarker and potential therapeutic target, Dis. Markers 2020 (2020) 8892312, https://doi.org/10.1155/2020/8892312.

[28] Q. Liu, X. Wang, Effect of TRPV2 cation channels on the proliferation, migration and invasion of 5637 bladder cancer cells, Exp. Ther. Med. 6 (5) (2013) 1277–1282, https://doi.org/10.3892/etm.2013.1301.

[29] H. Bai, H. Zhu, Q. Yan, X. Shen, X. Lu, J. Wang, J. Li, L. Chen, TRPV2-induced Ca(2+)-calcineurin-NFAT signaling regulates differentiation of osteoclast in multiple myeloma, Cell Commun. Signal. 16 (1) (2018) 68, https://doi.org/10.1186/s12964-018-0280-8.

[30] M. Monet, V. Lehen'kyi, F. Gackiere, V. Firlej, M. Vandenberghe, M. Roudbaraki, D. Gkika, A. Pourtier, G. Bidaux, C. Slomianny, P. Delcourt, F. Rassendren, J. P. Bergerat, J. Ceraline, F. Cabon, S. Humez, N. Prevarskaya, Role of cationic channel TRPV2 in promoting prostate cancer migration and progression to androgen resistance, Cancer Res. 70 (3) (2010) 1225–1235, https://doi.org/10.1158/0008-5472.CAN-09-2205.

[31] D. D'Arcangelo, F. Scatozza, C. Giampietri, P. Marchetti, F. Facchiano, A. Facchiano, Ion Channel expression in human melanoma samples: in silico identification and experimental validation of molecular targets, Cancers 11 (4) (2019), https://doi.org/10.3390/cancers11040446.

[32] J. Lu, G. Getz, E.A. Miska, E. Alvarez-Saavedra, J. Lamb, D. Peck, A. Sweet-Cordero, B.L. Ebert, R.H. Mak, A.A. Ferrando, J.R. Downing, T. Jacks, H.R. Horvitz, T. R. Golub, MicroRNA expression profiles classify human cancers, Nature 435 (7043) (2005) 834–838, https://doi.org/10.1038/nature03702.

[33] M. Dillhoff, J. Liu, W. Frankel, C. Croce, M. Bloomston, MicroRNA-21 is overexpressed in pancreatic cancer and a potential predictor of survival, J. Gastrointest. Surg. 12 (12) (2008) 2171–2176, https://doi.org/10.1007/s11605-008-0584-x.

[34] J. Wang, J. Wu, Role of miR-155 in breast cancer, Front. Biosci. 17 (6) (2012) 2350–2355, https://doi.org/10.2741/4056.

[35] Z. Wang, T.E. Li, M. Chen, J.J. Pan, K.W. Shen, miR-106b-5p contributes to the lung metastasis of breast cancer via targeting CNN1 and regulating Rho/ROCK1 pathway, Aging (Albany NY) 12 (2) (2020) 1867–1887, https://doi.org/10.18632/aging.102719.

[36] H. Wang, Y. Wang, Q. Du, P. Lu, H. Fan, J. Lu, R. Hu, Inflammasome-independent NLRP3 is required for epithelial-mesenchymal transition in colon cancer cells, Exp. Cell Res. 342 (2) (2016) 184–192, https://doi.org/10.1016/j.yexcr.2016.03.009.

[37] D. Xu, Y. Zhou, X. Xie, L. He, J. Ding, S. Pang, B. Shen, C. Zhou, Inhibitory effects of canagliflozin on pancreatic cancer are mediated via the downregulation of glucose transporter-1 and lactate dehydrogenase A, Int. J. Oncol. 57 (5) (2020) 1223–1233, https://doi.org/10.3892/ijo.2020.5120.

[38] B. Liu, X. Deng, Q. Jiang, G. Li, J. Zhang, N. Zhang, S. Xin, K. Xu, Scoparone improves hepatic inflammation and autophagy in mice with nonalcoholic steatohepatitis by regulating the ROS/P38/Nrf2 axis and PI3K/AKT/mTOR pathway in macrophages, Biomed. Pharmacother. 125 (2020) 109895, https://doi.org/10.1016/j.biopha.2020.109895.

[39] N. Schaft, J. Dorrie, G. Schuler, B. Schuler-Thurner, H. Sallam, S. Klein, G. Eisenberg, S. Frankenburg, M. Lotem, A. Khatib, The future of affordable cancer immunotherapy, Front. Immunol. 14 (2023) 1248867, https://doi.org/10.3389/fimmu.2023.1248867.

[40] L. Chen, W. Xue, J. Cao, S. Zhang, Y. Zeng, L. Ma, X. Qian, Q. Wen, Y. Hong, Z. Shi, Y. Xu, TiSe(2)-mediated sonodynamic and checkpoint blockade combined immunotherapy in hypoxic pancreatic cancer, J. Nanobiotechnol. 20 (1) (2022) 453, https://doi.org/10.1186/s12951-022-01659-4.

[41] S. Feske, H. Wulff, E.Y. Skolnik, Ion channels in innate and adaptive immunity, Annu. Rev. Immunol. 33 (2015) 291–353, https://doi.org/10.1146/annurev-immunol-032414-112212.
[42] F. Lefranc, Transient receptor potential (TRP) ion channels involved in malignant glioma cell death and therapeutic perspectives, Front. Cell Dev. Biol. 9 (2021) 618961, https://doi.org/10.3389/fcell.2021.618961.
[43] Q. Chen, H. Zhao, J. Hu, A robust six-gene prognostic signature based on two prognostic subtypes constructed by chromatin regulators is correlated with immunological features and therapeutic response in lung adenocarcinoma, Aging (Albany NY) 15 (21) (2023) 12330–12368, https://doi.org/10.18632/aging.205183.